2060 J. Phys. Chem. A **1999,** *103,* 2060−2065

Theoretical Investigation of the Reaction of $O(^3P)$ with CH_2Cl

Baoshan Wang, Hua Hou, and Yueshu Gu*

School of Chemistry, Shandong University, Jinan, 250100, China

Received: November 4, 1998; In Final Form: January 15, 1999

The reaction of oxygen atom with chlorinated methyl radical has been studied using the G2MP2 level of theory. The computation reveals an association−elimination mechanism. The addition reaction of $O(^3P)$ with CH_2Cl proceeds to the formation of an energy-rich intermediate OCH_2Cl^*. Four product channels of OCH_2Cl^* are found: H + CHClO, Cl + CH_2O, CHClOH, and H_2 + ClCO. The isomer CHClOH also has four product channels: H + CHClO, HCl + HCO, H_2 + ClCO, and OH + CHCl. On the basis of this ab initio potential energy surface and the experimental rate constant at 297 K, the kinetics of the title reaction have been calculated by a "loose transition-state" model and RRKM theory. The overall rate constants can be fitted to a double-exponential formula $k(T) = (1.51 \pm 0.01) \times 10^{-10} \exp[(1.36 \pm 0.01)\ \mathrm{kJ\ mol^{-1}}/(RT)] + (2.23 \pm 0.09) \times 10^{-10} \exp[(-27.48 \pm 0.73)\ \mathrm{kJ\ mol^{-1}}/(RT)]\ \mathrm{cm^3\ molecule^{-1}\ s^{-1}}$ over the temperature range 250−2000 K. The energy-specific rate constants of the unimolecular decomposition of the activated adduct OCH_2Cl^* are used to estimate the branching ratio. The production of H + CHClO is the major reaction channel, and the production of Cl + CH_2O is the minor reaction channel.

I. Introduction

Incineration is a broadly applicable and effective treatment method for the management of hazardous chlorinated hydrocarbons wastes in which the potentially toxic byproducts such as chlorinated methyl radicals are generated.[1,2] Under typical fuel-lean combustion conditions, the thermally stable chlorinated methyl radicals and the rich $O(^3P)$ atoms can undergo chemical reaction to a significant extent.[3,4]

The reaction of $O(^3P)$ with CH_2Cl is also important in the stratosphere because it generates chlorine atoms. It is well-known that the Cl atom takes part in the process of the catalytic destruction of ozone.[5,6]

The kinetics of the reaction of $O(^3P)$ with CH_2Cl were investigated by Seetula et al. using a heatable tubular reactor coupled to a photoionization mass spectrometer.[4] Several important results were reported. (1) The rate constant is quite large, within an order of magnitude of the gas kinetic collision number. (2) The rate constant is found to be pressure-independent and to exhibit a negative temperature dependence over the range 297−823 K: $k(T) = (1.49 \pm 0.35) \times 10^{-10} \exp[(1.46 \pm 0.38)\ \mathrm{kJ\ mol^{-1}}/(RT)]\ \mathrm{cm^3\ molecule^{-1}\ s^{-1}}$. (3) CHClO is the major product, and CH_2O is the minor product. Up to now, there are no any theoretical studies of this important reaction.

In this paper we have studied the reaction of $O(^3P)$ with CH_2Cl using ab initio calculations. The potential energy surface is explored at the G2MP2 level of theory, and the reaction mechanism is illustrated in detail. On the basis of the ab initio results, the rapid rate constants are deduced by the "loose transition state" model through fitting the experimental value at 297 K. The relative yields of various products are estimated by RRKM theory.

II. Computation Methods

Ab initio calculations are carried out using Gaussian 94 programs.[7] The inexpensive and reliable G2MP2 theory[8] is used to explore the potential energy surface for the reaction of $O(^3P)$ with CH_2Cl. The geometries of reactants, intermediates, transition states, and products are optimized at the UMP2(full) level of theory with the standard 6-31G(d) basis set. The vibrational frequencies are obtained at the same level in order to determine the nature of different stationary points and the zero-point-energy (ZPE) corrections (scaled by 0.93) to eliminate known systematic errors.[9] All the stationary points have been identified for the minimum (number of imaginary frequencies NIMAG = 0) or the transition state (NIMAG = 1). Then a series of single-point energies are calculated at UMP2/6-311G(d,p), QCISD(T)/6-311G(d,p), and UMP2/6-311+G(3df,2p) levels. Finally, the G2MP2 total energy is given by

$$E(\mathrm{G2MP2}) = E[(\mathrm{QCISD(T)/6\text{-}311G(d,p)})] + \Delta_{\mathrm{MP2}} + \mathrm{HLC} + E(\mathrm{ZPE})$$

where $\Delta_{\mathrm{MP2}} = E[\mathrm{MP2/6\text{-}311{+}G(3df,2p)}] - E[\mathrm{MP2/6\text{-}311G(d,p)}]$. HLC is a higher level correction, HLC $= -0.00019n_\alpha - 0.00481n_\beta$, and n_α and n_β are the number of α and β valence electrons, respectively.

III. Results and Discussion

The optimized geometries of various stationary points are shown in Figure 1. The corresponding frequencies and the energies are listed in Tables 1 and 2, respectively. The overall energetic profile based on the G2MP2 energies for the reaction of $O(^3P)$ + CH_2Cl is shown in Figure 2.

1. Reaction Mechanism. An association−elimination mechanism for the reaction of $O(^3P)$ with CH_2Cl is obvious, as shown in Figure 2. $O(^3P)$ atom attacks the radical center of CH_2Cl to form an intermediate OCH_2Cl^* (denoted as IM1). This process is found to be a barrierless association. The reaction takes place as the reactants are approaching each other to interact on an attractive potential energy surface. The adduct IM1 has C_s symmetry, $^2A''$ electronic ground state. The association reaction of $O(^3P)$ + CH_2Cl is highly exothermic by 91.75 kcal/mol at

---

* Corresponding author. E-mail: guojz@icm.sdu.edu.cn.

10.1021/jp984306s CCC: $18.00

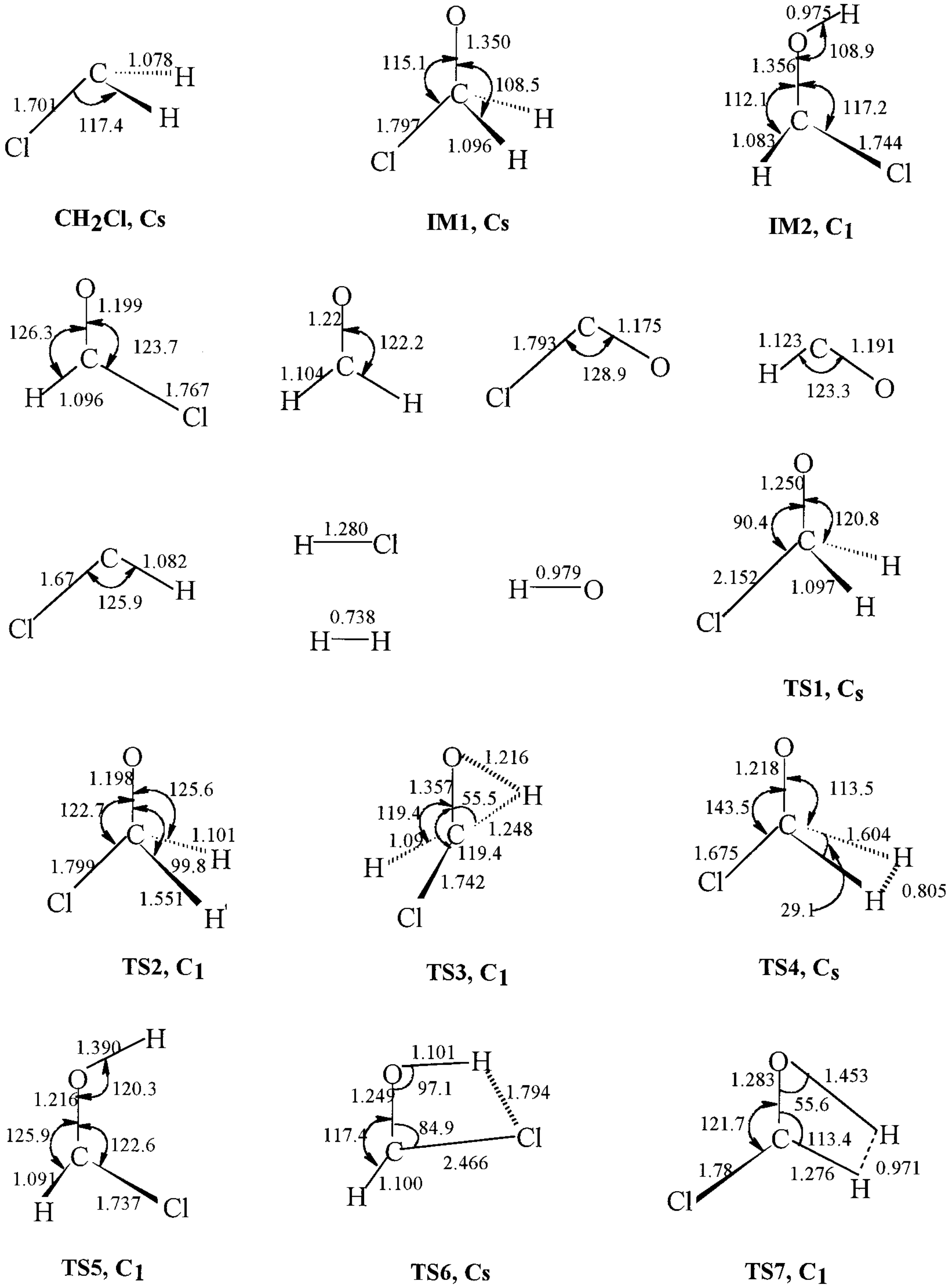

CH$_2$Cl, Cs **IM1, Cs** **IM2, C$_1$**

TS1, C$_s$

TS2, C$_1$ **TS3, C$_1$** **TS4, C$_s$**

TS5, C$_1$ **TS6, Cs** **TS7, C$_1$**

Figure 1. UMP2(full)/6-31G(d) optimized geometies of the various isomers of the reaction O(^{3}P) + CH$_2$Cl. Bond lengths are in angstroms and angles in degree.

the G2MP2 level of theory. It shows that IM1 is a short-lived activated complex. The heat of reaction is available for the rapid dissociation and isomerization reactions, which lead to various possible products.

Four product channels of IM1 have been found. The most favorable two paths are IM1 → Cl + CH$_2$O via the C−Cl cleavage transition state (TS1) and IM1 → H + CHClO via the C−H cleavage transition state (TS2). The barrier heights of TS1 and TS2 relative to IM1 are 11.20 and 18.20 kcal/mol, respectively. TS1 has C_s symmetry ($^2A''$ state). The breaking C−Cl bond is 0.35 Å longer than that of IM1. The forming "CH$_2$O" part is very similar to the geometry of the final product CH$_2$O. TS2 has C_1 symmetry. The breaking C−H bond is elongated from 1.096 Å in IM1 to 1.551 Å in TS2. C−O bond is shortened by 0.15 Å and is close to the C−O bond in the final product CHClO. Obviously, both TS1 and TS2 have productlike structures; i.e., they are later barriers. Because these two channels are highly exothermic by 87.0 and 83.0 kcal/mol, respectively, the polyatomic products CH$_2$O and CHClO can be internally excited.

The next pathway involves the isomerization of IM1 in which one of the H atoms on the C atom is shifted to the O atom to form another intermediate CHClOH (IM2) via a three-membered ring transition state TS3. The isomerization barrier height is 28.79 kcal/mol, which is 10.59 kcal/mol higher than TS2. From IM1 to IM2, C−Cl and C−H bonds become slightly short while

TABLE 1: Scaled UMP2(full)/6-31G(d) Harmonic Vibrational Frequencies of the Reactants, Products, Adducts, and Transition States

species	frequencies (cm^{-1})									ZPE (kcal mol^{-1})
CH_2Cl	310	822	984	1391	3041	3181				13.95
CH_2O	1164	1206	1474	1666	2801	2868				15.90
CHClO	438	720	904	1306	1684	2932				11.44
HCO	1056	1879	2561							7.91
ClCO	356	603	1860							4.00
CHCl	855	977	3073							6.98
HCl	2835									4.09
OH	3478									5.02
H_2	4215									6.05
IM1	382	687	696	1043	1054	1287	1339	2870	2932	17.58
IM2	360	437	701	827	1123	1217	1326	3050	3484	17.95
TS1	684i[a]	248	721	995	1178	1346	1522	2868	2959	16.93
TS2	1755i	406	589	640	693	1102	1273	1646	2866	13.21
TS3	2153i	392	616	739	919	1149	1257	2438	2980	14.97
TS4	1041i	454	565	704	788	898	1750	2487	3086	15.35
TS5	2618i	278	463	696	760	895	1309	1663	2979	12.93
TS6	1059i	185	336	581	1079	1218	1470	1863	2873	13.76
TS7	1868i	378	476	615	650	1049	1426	1837	2188	12.28

[a] i represents imaginary frequency.

TABLE 2: Total Energies and the Relative Energies of Various Species[a]

species	UMP2 /6-311G(d,p)	UMP2/6-311+G(3df,2p)	UQCISD(T) /6-311G(d,p)	G2MP2	ΔE	ΔH[b]
O + CH_2Cl	−573.679 37	−573.793 31	−573.732 50	−573.864 85	0.0	
Cl + CH_2O	−573.820 18	−573.939 54	−573.893 89	−574.003 48	−86.99	−85.0
H + CHClO	−573.808 25	−573.934 94	−573.843 43	−573.997 12	−83.00	−82.7
H_2 + ClCO	−573.820 90	−573.946 11	−573.867 35	−574.018 14	−96.19	−92.9
HCl + HCO	−573.837 57	−573.959 36	−573.879 94	−574.027 93	−102.33	−102.0
OH + CHCl	−573.663 09	−573.784 19	−573.714 41	−573.856 99	4.93	
IM1	−573.818 76	−573.944 27	−573.868 37	−574.011 06	−91.75	
IM2	−573.939 71	−573.969 19	−573.881 73	−574.027 86	−102.29	
TS1	−573.788 25	−573.915 06	−573.848 48	−573.993 22	−80.55	
TS2	−573.775 77	−573.904 98	−573.828 66	−573.982 06	−73.55	
TS3	−573.767 62	−573.897 51	−573.813 99	−573.965 18	−62.96	
TS4	−573.714 24	−573.848 22	−573.758 44	−573.913 16	−30.31	
TS5	−573.767 60	−573.897 19	−573.819 74	−573.973 91	−68.44	
TS6	−573.768 27	−573.894 48	−573.814 66	−573.964 18	−62.33	
TS7	−573.706 60	−573.840 41	−573.748 23	−573.907 58	−26.81	

[a] Total energies are in hartree; relative energies are in kcal/mol. [b] Enthalpy of formation at 0 K in ref 10 is used.

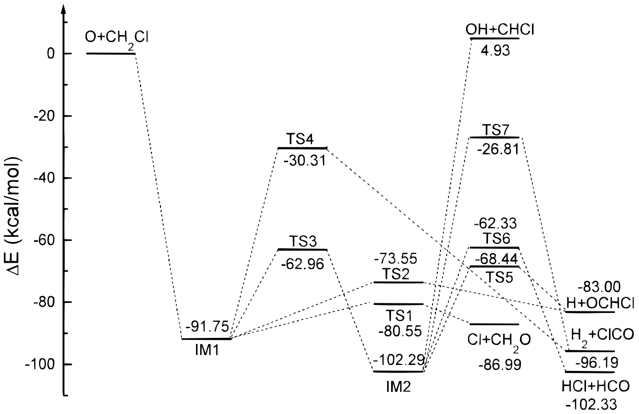

Figure 2. Overall profile of potential energy surface for the reaction of O(^{3}P) with CH_2Cl calculated at G2MP2 level of theory.

the C−O bond stays almost constant. The transition state (TS3) for this process has C_1 symmetry. The breaking C−H bond is 1.248 Å. The forming O−H bond is 1.216 Å. The product CHClOH is a trans structure with C_1 symmetry.

The fourth possible product channel is the three-center decomposition of IM1, forming H_2 + ClCO via transition state TS4. The barrier is as high as 61.44 kcal/mol above IM1 because of the strong repulsion of the three-membered ring, but it is still below the reactants O + CH_2Cl. Two C−H bonds in the IM1 stretch simultaneously to 1.604 Å. The forming H−H bond is 0.805 Å in the transition state TS4, which is only 0.067 Å longer than the equilibrium bond length of the final product H_2. Thus, TS4 is a later barrier. The other part “ClCO” in TS4 has a shorter C−Cl bond, a longer C−O bond, and a larger angle ClCO than their equilibrium values.

In principle, it is possible that another three-center decomposition path of IM1 to form HCl + HCO can occur. This process is the most exothermic channel in the reaction of O(^{3}P) + CH_2Cl ($\Delta H_0{}^0 = -102.33$ kcal/mol). However, neither HCl nor HCO is detected in the experiment.[4] Thus, if HCl + HCO are formed directly from IM1, a high activation barrier, which is at least similar to TS4, must be involved. Unfortunately, all our attempts to locate the transition state for this process proved futile at the UMP2(full)/6-31G(d) level with the Berny algorithm in Gaussian 94. Stretching C−H and C−Cl bonds and reducing the H−C−Cl angle simultaneously to make the forming H−Cl bond distance to be various values between the equilibrium HCl bond length (1.28 Å) and the H−Cl distance in IM1 (2.37 Å) invariably leads to the optimized structures of TS1 or TS2, or the H-abstraction transition states of the reactions of Cl + CH_2O and H + CHClO.

It can be seen from Figure 2 that IM2 is 11.54 kcal/mol more stable than IM1; i.e., IM2 has higher internal energy. Many decomposition channels of IM2 would be open. The most feasible decomposition channel of IM2 is the formation of H

+ CHClO via a C−H bond fission transition state TS5 with the lowest barrier (33.85 kcal/mol relative to IM2). The C−H bond is elongated by 0.41 Å in TS5, while the C−O bond is shortened by 0.15 Å. The second product channel is breaking C−Cl and O−H bonds simultaneously, forming the final products HCl + HCO via a four-membered ring transition state TS6. The forming H−Cl bond length in TS6 is 1.794 Å, which is 0.51 Å longer than its equilibrium value. So this transition state is more reactantlike. Another four-center decomposition of IM2 forms the products H_2 + ClCO via the transition state TS7. The forming H−H bond (0.971 Å) in TS7 is about 0.23 Å longer than the equilibrium bond length of H_2. Similar to TS6, TS7 also is an early barrier. It is interesting to note that the H−H bond in the three-center transition state TS4 is about 0.17 Å shorter than that in the four-center transition state TS7. It is obvious in Figure 2 that both of the channels to form H_2 + ClCO have relatively high barriers.

The fission of C−O bond in IM2 generates the products OH and CHCl without a pronounced barrier. This is an endothermic path of the reaction O(^{3}P) + CH_2Cl ($\Delta H_0{}^0 = 4.93$ kcal/mol). The energy of OH + CHCl is 107.22 kcal/mol higher than that of IM2. Thus, this channel cannot occur to any extent.

2. Kinetic Analysis. The calculated heats of reaction for various product channels at 0 K are in reasonable agreement with the experimental values,[10] as listed in Table 2. The average deviation is 1.5 kcal/mol. It implies that the present ab initio G2MP2 potential energy surface is high quality. Therefore, the kinetics of O(^{3}P) + CH_2Cl can be deduced reasonably on the basis of this potential energy surface.

(1) Overall Rate Constant. Seen from the energetic profile for the reaction of O(^{3}P) + CH_2Cl (Figure 2), the adduct IM1 has high internal energy (91.75 kcal/mol) and thus a short lifetime. Once IM1 is formed, the forward reaction is much faster than the redissociation of the complex such that the barrierless association of the O atom with the CH_2Cl radical becomes the rate-limiting step. The resulting rate constant is pressure-independent and only temperature-dependent, just as measured in the experiments.[4,11−14]

For the present barrierless radical−radical association reaction of O(^{3}P) with CH_2Cl, the direct dynamic methods are necessary to obtain accurate kinetic information. For instance, the canonical variational transition-state theory,[15−20] which amounts to locating the transition structure with the highest free energy as the bottleneck of the barrierless entrance reaction, is a more appealing method. However, this type of calculation cannot be archived at present because of the difficulties in programming and computational facilities. So a simpler but more empirical method, the "loose transition-state" model,[21,22] is used to simulate the overall rate constants for the reaction of O(^{3}P) with CH_2Cl. Further work is in progress.

By use of the "loose transition-state" model, the overall rate constant can be obtained directly as

$$k(T) = l(kT/h)(Q^{\ddagger}/(Q_AQ_B)) \qquad (1)$$

where l is the reaction path degeneracy, k and h are the Boltzmann and Planck constants, respectively, and T is the temperature of interest. $Q^{\ddagger}$, Q_A, and Q_B represent the total partition functions of the loose transition state, the reactants O(^{3}P) and CH_2Cl, respectively. It should be noted that the reactant O(^{3}P) is an atom, it has no rotational and vibrational partition functions. But O(^{3}P) has a large electronic partition function due to the spin−orbital splitting of the ^{3}P level, $Q_{A,e} = 5.0 + 3.0\exp(-158.5\ \text{cm}^{-1}/(RT)) + \exp(-226.5\ \text{cm}^{-1}/(RT))$.[13,23]

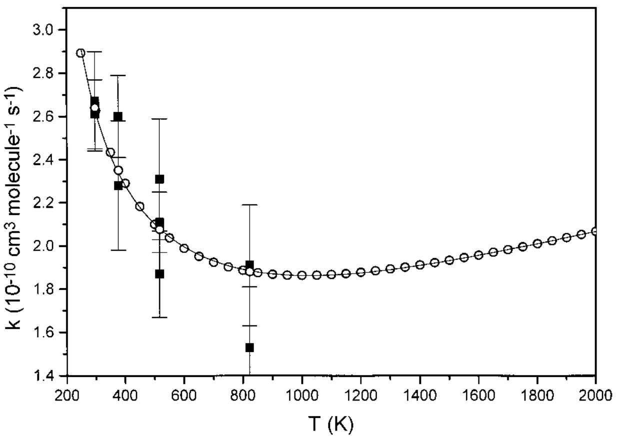

Figure 3. Calculated overall rate constant for the reaction of O(^{3}P) + CH_2Cl. The used parameters are the following: I of CH_2Cl. 6.56, 113.87, 120.00 (amu); I of IM1, 38.21, 310.33, 337.04 (amu). The free internal rotational constant is 2.08 cm^{-1}. The vibrational frequencies of the loose transition state are those of CH_2Cl and 1050 cm^{-1} (see text for details). The hollow circles are the calculated data. Solid squares are the experimental values from ref 4. The solid line is the result fitted by a double-exponential function.

Because the "loose transition state" for the association reaction of O(^{3}P) with CH_2Cl cannot be obtained using the ab initio calculation, some structure information must be assumed to obtain the necessary parameters for evaluating the rate constant by eq 1.[24−26] To obtain the vibrational and rotational partition functions of the "loose transition state", its vibrational frequencies and moment of inertia should be determined first. The external moment of inertia of the "loose transition state" is thought to be temperature-dependent, i.e., $I^{\ddagger}/I = (6D_e/(RT))^{1/3}$, where $D_e = 91.75$ kcal/mol. $I^{\ddagger}$ represents the moment of inertia ($I^{\ddagger}{}_a$, $I^{\ddagger}{}_b$) of "the loose transition state". I has the same meaning but for the intermediate IM1. $I^{\ddagger}{}_c$ is set to be I_c.

According to the conventional "loose transition-state" model, the vibrational frequencies of the "loose transition state" are assumed to be those of the reactant CH_2Cl. In addition, one of the remaining three degrees of freedom should be considered as the reaction coordinate. The other two degrees can be assumed to be either two low-frequency vibrations or two internal rotations. The necessary vibrational frequencies or rotational constants are obtained through fitting the known experimental rate constant at $T = 297$K, $k = 2.64 \times 10^{-10}$ cm^3 molecule^{-1} s^{-1}. Then the rate constants over a wide range of temperature can be extrapolated using these best-fitted parameters. Although the rapid rate constant can be simulated by this method, the rate constants increase with the temperature. The negative temperature dependence observed in the experiment cannot be obtained.

Consequently, another assumption has to be made: besides the six vibrations of the reactant CH_2Cl, one free internal rotation corresponding to the rotational motion of CH_2Cl about the forming C−O bond and one vibration representing the soft bending vibrational motion of the bonds being formed are introduced in eq 1. After fitting the experimental rate constant at 297 K, the calculated rate constants versus the temperature are shown in Figure 3. It is obvious that the calculated data are in quite good agreement with the experimental values over the temperature range 297−823 K.[4]

At the lower temperature, the rate constants show a negative temperature dependence. According to eq 1, two aspects lead to the negative temperature dependence. One is the spin−orbital splitting of O(^{3}P). The other is the temperature-dependent moment of inertia, i.e., the position of the effective barrier that changes with the temperature. As the temperature increases, these two factors become less and less important. Therefore, the rate constants become flat and increase slightly, showing a positive activation energy. This is the characteristic of the radical−radical capture-limited reactions.[14,27] Those rate constants at higher temperature are waiting for the experimental measurements for comparison. The calculated rate constants can be well fitted using a double-exponential formula over a temperature range of 250−2000 K:

$$k(T) = (1.51 \pm 0.01) \times 10^{-10} \exp[(1.36 \pm 0.01)\ \mathrm{kJ\ mol^{-1}}/(RT)] + (2.23 \pm 0.09) \times 10^{-10} \exp[(-27.48 \pm 0.73)\ \mathrm{kJ\ mol^{-1}}/(RT)]\ \mathrm{cm^3\ molecule^{-1}\ s^{-1}}$$

The first term is in good agreement with the Arrhenius equation obtained by Seetula et al. over 297−823 K:[4]

$$k(T) = (1.49 \pm 0.35) \times 10^{-10} \exp[(1.46 \pm 0.38)\ \mathrm{kJ\ mol^{-1}}/(RT)]\ \mathrm{cm^3\ molecule^{-1}\ s^{-1}}$$

However, we must remember that the rate constants obtained by the "loose transition-state" model are very empirical. This type of simulation only is qualitatively reasonable.

(2) Energy-Specific Rate Constants. At low pressure, the collision deactivation rate of the energy-rich adduct OCH_2Cl is relatively small. The relative yields of various products in the reaction of $O(^3P)$ with CH_2Cl are determined by the unimolecular decomposition rate of OCH_2Cl. The ab initio calculated four product channels of the decomposition of OCH_2Cl are considered, namely,

$$\begin{aligned} OCH_2Cl &\rightarrow Cl + CH_2O && \text{(I)} \\ &\rightarrow H + CHClO && \text{(II)} \\ &\rightarrow CHClOH && \text{(III)} \\ &\rightarrow H_2 + ClCO && \text{(IV)} \end{aligned}$$

The energy-specific rate constants for unimolecular decomposition of the adduct OCH_2Cl are given by RRKM theory using a simple treatment of adiabatic rotations as[24−26,28]

$$k_i(E) = l_i \left(\frac{I_a^{\ddagger} I_b^{\ddagger} I_c^{\ddagger}}{I_a I_b I_c} \right)^{1/2} \frac{G_i(E - E_i^{\ddagger})}{hN(E)} \tag{2}$$

where l_i is the reaction path degeneracy for channel i, h is Planck constant, $N(E)$ is the density of vibrational state of OCH_2Cl at internal energy E, and $G_i(E - E_i^{\ddagger})$ is the sum of accessible vibrational states of the transition states for channel i at energy $E - E_i^{\ddagger}$, where $E_i^{\ddagger}$ is the barrier height of the transition state for channel i. $(I_a^{\ddagger} I_b^{\ddagger} I_c^{\ddagger})$ and $(I_a I_b I_c)$ is the product of three overall moment of inertia for the transition state i and the adduct OCH_2Cl. Owing to the decomposition transition states of OCH_2Cl are all "tight", $N(E)$ can be deduced easily by the steepest decent method[28] and $G_i(E - E_i^{\ddagger})$ can be calculated using the Beyer−Swinehart algorithm.[29]

The RRKM rate constants for four dissociation channels I−IV as a function of the internal energy E are depicted in Figure 4. The reaction rate for channel I, k_1, is faster at low energies than for other three channels because of the lower barrier height of channel I (see Figure 2). At energies greater than 40 kcal/mol, the reaction rate k_2 for channel II gives a larger value than for channel I, since the vibrational frequencies of channel II are smaller than those of channel I (see Table 1), which results in a larger sum of states for channel II. At energies greater than 130 kcal/mol, the reaction rate k_3 for channel 3 also becomes higher than for channel I because of the same reason. Within the range of the internal energy considered in this study, the one for channel IV is much smaller than those of k_1, k_2, and k_3 because of the highest activation energy of channel IV.

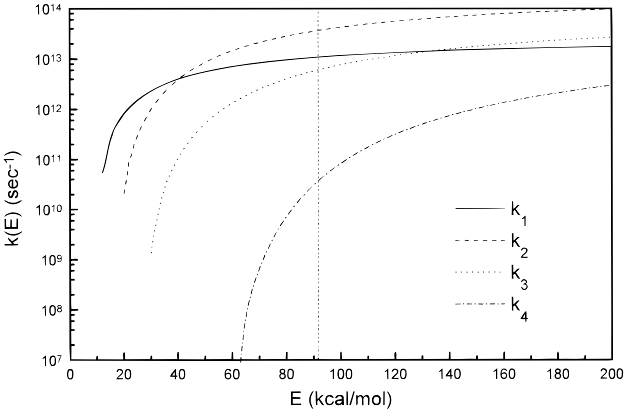

Figure 4. Dependence of the energy-specific rate constant on internal energy for the unimolecular dissociation of OCH_2Cl.

The branching ratio of the productions can be estimated by the microcanonical rate constants at $E = E_R$ (E_R is the maximum internal energy that IM1 can obtain, i.e., 91.75 kcal/mol, and as indicated in ref 11, the implied neglect of thermal energy of IM1 is justified at low to moderate temperature). The calculated microcanonical rate constants for these four channels are 1.1×10^{13}, 3.6×10^{13}, 6.0×10^{12}, and $3.8 \times 10^{10}\ s^{-1}$, respectively. The relative ratio of rate constants is 1.0/3.3/0.54/0.0034. It is obvious that the reaction rate for channel II is the fastest. Thus, the formation of H + CHClO is the major product channel. The sum of reaction rates for channels I and III is about half of that for channel II. The rate constant for channel III is about half of that for channel I. Both $Cl + CH_2O$ and CHClOH are minor products. Channel IV has the smallest rate constant. The product for channel IV, $H_2 + ClCO$, should not be detectable.

As indicated by the referee, the sum of the above four rate constants is $5.3 \times 10^{13}\ s^{-1}$, which means that the lifetime of the activated OCH_2Cl^* intermediate would be only 2.0×10^{-14} s. For such a short lifetime, RRKM theory is no longer suitable, since the reaction becomes nonergodic. Therefore, the branching ratio obtained by RRKM theory cannot be considered as a quantitative conclusion but rather as a qualitative estimation. Our results are consistent with the findings of Seetula et al., who reported that CHClO is a major product and CH_2O is a minor product through comparison of the ion signals of the products.[4]

IV. Conclusions

The following conclusions can be drawn from this study.

(1) G2MP2 theory is used to explore the potential energy surface for the reaction of $O(^3P)$ with CH_2Cl. Agreement of the calculated heats of reaction at 0 K with the available experimental data implies that the calculated G2MP2 potential energy surface is high quality.

(2) The detailed association−elimination mechanism of the reaction $O(^3P) + CH_2Cl$ is presented. Two intermediates and seven transition states are located along the reaction paths.

(3) The "loose transition-state" model is applied to obtain the rate constant for the reaction of $O(^3P) + CH_2Cl$. The essential parameters used are obtained through fitting the experimental value at 297 K. The overall rate constant over the

range 250−2000 K can be fitted by a double-exponential formula:

$$k(T) = (1.51 \pm 0.01) \times 10^{-10} \exp[(1.36 \pm 0.01)\ \text{kJ mol}^{-1}/(RT)] + (2.23 \pm 0.09) \times 10^{-10} \exp[(-27.48 \pm 0.73)\ \text{kJ mol}^{-1}/(RT)]\ \text{cm}^3\ \text{molecule}^{-1}\ \text{s}^{-1}$$

(4) The branching ratio of the productions is estimated qualitatively by the energy-specific rate constants for four unimolecular decomposition of OCH$_2$Cl with RRKM calculation. It is shown that H + CHClO are the major products and Cl + CH$_2$O are the minor products.

Acknowledgment. This work is supported by the National Natural Science Foundation of China. The authors express our gratitude to the referees for their valuable comments.

References and Notes

(1) Senkan, S. M. *Environ. Sci. Technol*. **1988**, *22*, 2368.

(2) Altwicker, E. R.; Schonberg, J. S.; Konduri, R. K. N. Y.; Milligan, M. S. *Hazard. Waste Hazard. Mater.* **1990**, *7*, 73.

(3) Seetula, J. A.; Slagle, I. R.; Gutman, D.; Senkan, S. M. *Chem. Phys. Lett.* **1996**, *252*, 299.

(4) Seetula, J. A.; Slager, I. R. *Chem. Phys. Lett.* **1997**, *277*, 381.

(5) Cicerone, J. R. *Science* **1987**, *237*, 35.

(6) Sridharan, V. C.; Klein, F. S.; Kaufman, F. *J. Chem. Phys.* **1985**, *82*, 592.

(7) Frisch, M. J.; Trucks, G. W.; Schlegel, H. B.; Gill, P. W. M.; Johnson, B. G.; Robb, M. A.; Cheeseman, J. R.; Keith, T. A.; Petersson, G. A.; Montgomery, J. A.; Raghavachari, K.; Allaham, M. A.; Zakrzewski, V. G.; Ortiz, J. V.; Foresman, J. B.; Cioslowski, J.; Stefanov, B. B.; Nanayakkara, A.; Challacombe, M.; Peng, C. Y.; Ayala, P. Y.; Chen, W.; Wong, M. W.; Andres, J. L.; Replogle, E. S.; Gomperts, R.; Martin, R. L.; Fox, D. J.; Binkley, J. S.; Defrees, D. J.; Baker, J.; Stewart, J. P.; Head-Gordon, M.; Gonzales, C.; Pople, J. A. *Gaussian 94*; Gaussian Inc.: Pittsburgh, PA, 1995.

(8) Curtiss, L. A.; Raghvachari, K.; Pople, J. A. *J. Chem. Phys.* **1993**, *98*, 1293.

(9) Hehre, W. J.; Radom, L.; Schleyer, P. V. R.; Pople, J. A. *Ab initio Molecular Orbital Theory*; John Wiley: New York, 1986.

(10) Boulch, D. L.; Cox, R. A.; Hampson, R. F.; Kerr, J. A., Jr.; Troe, J. *J. Phys. Chem. Ref. Data* **1980**, *9*, 466.

(11) Sumathi, R.; Peeters, J.; Nguyen, M. T. *Chem. Phys. Lett.* **1998**, *287*, 109.

(12) Gilbert, R. G.; Smith, S. C. *Theory of Unimolecular and Recombination Reactions*; Blackwell Scientific: Oxford, 1990.

(13) Smith, I. W. M. *Kinetics and dynamics of elementary gas reactions*; Butterworth: London, 1980.

(14) Thiesemann, H.; Taatjes, C. A. *Chem. Phys. Lett.* **1997**, *270*, 580.

(15) Mebel, A. M.; Morokuma, K.; Lin, M. C. *J. Phys. Chem.* **1995**, *99*, 1900.

(16) Mebel, A. M.; Diau, E. W. G.; Lin, M. C. Morokuma, K. *J. Am. Chem. Soc.* **1996**, *118*, 9759.

(17) Hsu, C. C.; Lin, M. C.; Mebel, A. M.; Melius, C. F. *J. Phys. Chem.* A **1997**, *101*, 60.

(18) Hsu, C. C.; Mebel, A. M.; Lin, M. C. *J. Chem. Phys.* **1996**, *105*, 2346.

(19) Chakraborty, D.; Park, J.; Lin, M. C. *Chem. Phys.* **1998**, *231*, 39.

(20) Garret, B. C.; Truhler, D. G. *J. Chem. Phys.* **1979**, *70*, 1593.

(21) Smith, G. P.; Golden, D. M. *Int. J. Chem. Kinet.* **1978**, *10*, 489.

(22) Berman, M. R.; Lin, M. C. *Chem. Phys.* **1983**, *82*, 435.

(23) Moore, C. E. *At. Energy Levels* **1971**, *1*, 45.

(24) Lin, M. C.; He, Y.; Melius, C. F. *J. Phys. Chem.* **1993**, *97*, 9124.

(25) Berman, M. R.; Lin, M. C. *J. Phys. Chem.* **1983**, *87*, 3933.

(26) Hsu, D. S. Y.; Shanb, W. M.; Creamer, T.; Gutaman, D.; Lin, M. C. *Ber. Bunsen-Ges. Phys. Chem.* **1983**, *87*, 909.

(27) Smith, I. W. M. *Int. J. Mass Spectrom. Ion Processes* **1995**, *149/150*, 231.

(28) Forst, W. *Theory of unimolecular reactions*; Academic Press: New York, 1973.

(29) Stein, S. E.; Rabinovitch, B. S. *J. Chem. Phys.* **1973**, *58*, 2438.